

Evaluating Stereoscopic Visualization for Predictive Rendering.

Fernando da Graça
Center for Robotics
MINES ParisTech,
PSL-Research University
60 Boulevard Saint
Michel
75006, Paris, France
fernando.graca@mines-
paristech.fr

Alexis Paljic
Centre for Robotics
MINES ParisTech,
PSL-Research University
60 Boulevard Saint
Michel
75006, Paris, France
alexis.paljic@mines-
paristech.fr

Emmanuelle Diaz
R&D Department,
Cognitive Science and
Human Factors
PSA Peugeot Citroën
2, route de Gisy
78943,
Vélizy-Villacoublay
Cedex, France
emmanuelle.diaz@mpsa.com

ABSTRACT

The context of this work is predictive rendering; our objective is to previsualize materials based on physical models within computer graphics simulations. In this work we focus on paints constituted of metallic flakes within a dielectric binder. We want to validate a "virtual material workshop" approach, where a user could change the composition and the microstructure of a virtual material, visualize its predicted appearance, and be able to compare it to an actual sample. To do so, our methodology is to start from Scanning Electron Microscopy (SEM) imaging measures on an actual sample that allowed us to characterize two metrics: flake size and flake density. A statistical model based on those measures was then integrated in our spectral rendering engine using raytracing and photon mapping, with an off axis-frustum method to generate stereoscopic images for binocular visualization. Our objective is twofold: 1) perceptually validate our physical model, we evaluate if the virtual metric perceptually corresponds to the real metric of the real samples; 2) evaluate the contribution of virtual reality techniques in the visualization of materials. To do so, we designed a user study comparing photographs of car paint samples and their virtual counterpart based on a design of experiments. The observers evaluated the visual correspondence of different virtual materials generated from microstructures with varying metric values. The results show a perceptual correspondence between real and virtual metrics. This result has a strong impact: it means that for a desired appearance the proposed models correctly predict the microstructure. The second result is that stereoscopy improves the metric correspondence, and the overall appearance score.

Keywords

virtual-reality, predictive rendering, visual perception, complex materials, metallic paints, microstructure, statistical model

1 INTRODUCTION

The study of visualization quality is a crucial step to accurately represent digital prototypes. Manufacturing departments understand this problematic, since they rely on digital representations of the end product to make critical choices about its final appearance. Furthermore, it gives them the freedom to comprehensively explore (simulate) a large variety of materials without

the need to manufacture the actual object. However, a correct representation of real materials still remains a challenging task. To this end, researchers focused on developing Predictive Rendering (PR) techniques to reduce the gap between the observations of a physical object and its virtual replica.

According to Wilkie et al. [1] PR, as opposed to believable rendering, is a field of research that aims at creating physically correct computer images [2, 3]. The objective is to predict the true visual appearance from a virtual reflectance model, which takes into consideration the physical parameters of the actual material. If such a tool was to be mastered, it would allow to design a virtual material and simulate its visual appearance iteratively. Then, when the desired appearance is obtained for the digital prototype, the actual equivalent object could be produced with the same set of param-

Permission to make digital or hard copies of all or part of this work for personal or classroom use is granted without fee provided that copies are not made or distributed for profit or commercial advantage and that copies bear this notice and the full citation on the first page. To copy otherwise, or to publish, to post on servers or to redistribute to lists, requires prior specific permission and/or a fee.

eters that were used as input for the virtual reflectance model. This process is meant to lead to better design decisions at a lower cost. Predictive rendering has a very strong potential in various application domains, ranging from manufacturing industries (automotive, aeronautics), cosmetics to architecture (material design).

On the other hand, complex materials such as automotive paints are very challenging to simulate, due to their spatially varying reflectance. To this end, we argue that VR tools are indispensable to fully explore the visual aspect of such materials. Virtual Reality is used in the industry for product design or industrial process validations. Through the use of stereoscopic displays, user motion capture, motion parallax, VR allows for a user to feel immersed in a 1:1 scale virtual environment, and to observe objects and interact with them. In particular, binocular vision and motion parallax are necessary to provide the human visual system with valuable depth and shape cues. These are key characteristics of VR that are necessary to ensure "human in the loop" simulations. In order to combine the physical and visual validity of Predictive Rendering and perception cues provided by Virtual Reality, the need for stereoscopy and motion parallax for predictive rendering simulations is being expressed by the industry.

Predictive rendering approaches require perceptual validations that take into account the human visual system in order to be valid. The field of research for such validations is large and we are only starting to draw the boundaries within which virtual material samples are representative of real material samples. Indeed, image quality perception can depend on a lot of parameters that appear at several stages of the process. One should, at least, consider the following: the human user (visual acuity, individual color perception, visual fatigue), the technical setup (display calibration, display resolution, luminance), the sensory motor inputs and outputs (use of stereoscopy, motion parallax, user's ability to manipulate the virtual material sample), and the rendering engine itself (light-matter interaction models, material models). In this context, this work is part of an iterative validation process in a research project of a predictive rendering engine in which the objective is to link microstructure and appearance. In this work, our objective is twofold: 1) evaluate the pertinence of a "virtual material workshop" approach where a user could change the composition and the microstructure of a virtual material, visualize its predicted appearance, and be able to compare it to an actual sample. To do so, we propose to use a microstructure model [4] based on measures of actual material samples presented in section 2.2; 2) evaluate the role of stereoscopy on perception of materials that depict binocular differences such as automotive paints with metallic flakes. For this purpose, our methodology evaluates, through a user study, the visual agreement between the observation of the com-

puter generated object and the actual object. We introduce a novel approach in Computer Graphics (CG) domain to render virtual materials by using the microstructure formulation of the real material, see figure 2.

We begin the paper with a survey of related work in section 1.1. In section 2 we describe the simulation of virtual automotive paints using a microstructure model. Then, in section 3 we describe the experimental setup of the virtual scene, and section 4 the design of experiment to evaluate the response of the observers. In the section 5 we present the results of the measured data. The experimental results are analyzed in the section 6. Finally, in section 7 we present our conclusions, and we address some aspects for future work to complement our findings.

1.1 Related Work

In this section, we first propose an overview of the existing CG (Computer Graphics) methods for computer generated images of materials with nano/macro inclusions such as car paints with flakes. We then explore the existing literature on the role of stereoscopy on the perception of surface aspect.

In the CG domain, several researches have proposed different methods to simulate car paint models. These models are based on Bidirectional Reflectance Distribution Function [5], which represents how the surface reflects the incident light at different angles. The distribution of the reflectance of the light can be captured by optical measurement devices [6]. Then, the obtained data is used to derive reflectance models that represent the appearance of the physical material [7]. In addition, we can also consider the Bidirectional surface scattering distribution function (BSSRDF) models [8] that takes into account the scattering of the incident beam of light in the interior of the material.

Generally speaking, we can distinguish two groups: analytical, and data-driven models. In the first, the user tweaks several parameters until he achieves a visual aspect that is similar to the real paint. Durikovic et al. [9] model the geometry of the flakes inside the paint film. Their system is capable of generating stereoscopic images, and it allows to define the parameters for the random distribution of the position of flakes and their orientation. The approach of Ershov et al. [10] is based on reverse engineering, the appearance attributes such gloss are added to the physical model by adjusting parameters. The inconvenient of these models is the amount of parameters that are necessary to represent the car paint appearance.

In the second approach, Günther et al. [11] developed an image based acquisition setup to measure the Bidirectional Reflectance Distribution Function (BRDF) of

a car paint. To this BRDF they add the sparkle simulation. The distribution of the the flakes is stored as a texture. Rump et al. [12] used a similar approach as the previous one. The difference is that, instead of using a sparkle simulation with the BRDF, they capture the spatially varying appearance (sparkle effect) using Bidirectional Texture Function (BTF) measurements. In addition, they store and simulate directional visual effects. Sung et al. [13] determine individual flake orientations in the car paint by using confocal laser scanning microscope. They capture the angular dependent reflectance using a goniometer. Then, they use these measurements to build a reflectance model. In the context of this work, we need to evaluate the perception limits in a VR environment, when the observer perceives the aspect of the reflectance models using binocular vision. A human observer perceives the binocular summation of the left and right image. In the combination of the two images, we can identify two cases binocular fusion and rivalry. In the first case, if two retinal points are sufficiently similar, a binocular combination occurs. In contrast, when two retinal points are very distinct, the observer perceives a fluctuation between the left and right images, that is, a failed fusion occurs. This phenomenon is known as binocular rivalry [14].

Most of the work was done on the role of stereoscopy for the perception of gloss. In the literature the gloss is defined to be a global property of the surface aspect [15, 16]. Glossy surfaces reflect the incident light to a particular outgoing direction, characterized by a specific angular interval. The perception of specular reflections is an important cue to evaluate the glossiness of the materials. In addition, there is an influence of binocular cues such as highlight disparities on the perception of gloss [17]. The experimental results of Wendt et al. [18] show an improvement of gloss perception when highlights cues disparities are taken into account. The experimental results of the work of G. Obein et al. [19] suggest also that the binocular vision helps for judgment of high gloss samples. They found that with binocular vision the sensitivity to gloss is higher than the monocular vision, for high gloss levels. Sakano et al. [20] examined the effects of the combination of self-motion and contingent retinal-image motion (motion parallax) on perceived glossiness. When the observer was able to move his head, a stronger glossiness was perceived than when both the observer and the stimulus were static. From their experimental results, they found that the glossiness under the monoscopic condition was underestimated compared to stereoscopic condition. The glossiness under static (head not moving) condition was underestimated compared to dynamic condition. Knill et al. [21] study the combination of different cues for slant perception. At low slants, observers use more the binocular cues than the texture. At slants of 50 and 70, the subjects do better slant judg-

ments using the texture information of the image. As the slant increases the observers give more attention to texture information.

2 MATERIAL SIMULATION

2.1 Physical Plate

This study focus on grey automotive paints with metallic flakes up to $30\mu\text{m}$. Figure1(a) shows a cross section of the studied actual sample of a car paint. Typically an automotive paint is made of four layers: clear coat, base coat, primer surface, and electrocoat. The metallic flakes are made of aluminum, and are distributed with different orientations on the primer surface of the plate at different depths, and the clear coat is transparent. The amount, distribution, and the orientation of the flakes are controlled by a milling machine. Due to their size, and orientation, these metallic pigments convey distinctive visual appearances to the object such as sparkle, and directional visual effects. At the macroscopic scale of visualization, the appearance of these nonuniform paints depend on the lighting conditions (directional/diffuse), distance and angle of observation, orientation, diameter, and density of the flakes [22, 23, 24]. The nanoscopic effects such as the chemical composition, rugosity and clustering effects of the flakes can also influence the visual appearance. In this work we only consider the macroscopic effects for which we use geometric optics models.

2.2 Stack Model

As for the models of the microstructure, we can distinguish two cases: a quasistatic, where the particles are smaller than the wavelength, consequently the human eye cannot perceive each particle. We can obtain the macroscopic visual aspect of the microstructure, which is visible by the human eye, by using homogenization methods on agglomerations of nanoscopic particles. In this work, we are interested in the second case, geometric optics, where the particle size is larger than electromagnetic visible wavelength, which is suitable to be directly used in our render engine. In this case the microstructure simulates the distribution of microscopic particles, such as metallic flakes, according to the analyses of the actual object. Morphology and statistical analysis of Scanning Electron Microscopy (SEM) images of real objects is used to create virtual microstructures that geometrically corresponds to the one of the real material. These microstructures are then used to simulate the optical behavior between the different particles. Secondly, it allows the user to modify the microstructure in order to tune the visual appearance keeping the physical feasibility, and therefore the manufacture of the virtual material, see figure 2. The stack model [4] used in our render engine distributes the metallic flakes on the surface. Though the complex

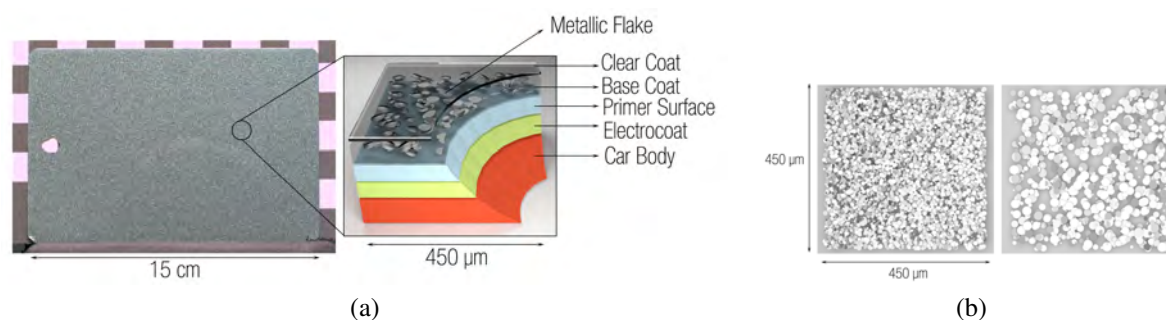


Figure 1: On the left of the image (a), an example of a real car paint plate with a diagram of a typical coating paint. The flakes have typically the shape of a disk with a diameter of $5\mu\text{m}$ to $50\mu\text{m}$, in the case of a car paint. The surface can contain rugosity and an interference film. The flakes are imbedded in the base coat with different orientations and at different depths. The figure (b) depicts two microstructures generated by the stack model. On the left a microstructure with metallic flakes of size $15\mu\text{m}$, and on the right with metallic flakes of size $30\mu\text{m}$.

geometry of a real metallic flake, the virtual metallic flakes were modeled with a flat cylinder shapes whose height and radius is parameterized, see figure 1(b). The statistical variation of dispersion, size, orientation is measured on the SEM images of the real plate using different morphological analyses. Then, the model simulates the clusters of flakes by using a 2D Poisson point process. Due to the large number of flakes on the surface. The stack model generates continuous microstructures of size $450\mu\text{m} \times 450\mu\text{m} \times 20.24\mu\text{m}$. The generation of plates with different flake densities and radius sizes is controlled by two parameters of the stack model. For each microstructure we have information about the radius size, the orientation, position, and amount of flakes. To generate a virtual plate with $15\text{cm} \times 10\text{cm}$, a set of 332×240 microstructures is necessary to fill the surface of the virtual plate. To avoid the large amount of geometry in our simulations, we could consider the usage of a set of textures encoding different types of information about the flakes, for instance the normal vector, and depth.

2.3 Rendering of the Virtual Model

For the optical simulation of the virtual object we used our spectral render engine raytracing with photon mapping. The scene was rendered within the visible spectrum interval $[380\text{nm} - 780\text{nm}]$ with a wavelength step of 5nm . This interval corresponds to the range of wavelengths that the human eye is sensitive. Then, we used a virtual scene with the same light conditions that were used in the real room. We associate for each plate the optical constants n and k of aluminium. In the virtual scene we used the spectrum of SOLUX 4700K light. The index of absorption was found in a prior experience with paired comparison. The observers were asked to evaluate which of the two virtual images was the closest to the photograph. The found absorption coefficient is $k = 6$. Furthermore, we noticed that the thickness and the absorption coefficient have an important role

in the brightness of the metallic flakes. We used a virtual plate with three layers. The base layer is a black surface to minimize the back-surface reflection. The second layer, the binder, contains the microstructure of the metallic flakes, which was generated by the stack model. Finally, the clear coat layer imparts a glossy appearance to the plate. The virtual samples were defined thanks to a design of experiments. We have two factors the flake size and the flake density. A surface response design was chosen in order to evaluate the influence of the main effects but also the potential non linear effects and the interaction between factors. 13 virtual samples were built following a central composite design with replicated centered points.

3 SETUP

In this section we describe the configuration of the virtual scene. Figure 3(a) represents the virtual scene used in the experiments. We used a directional isotropic light, which is emitted from the top. The virtual cameras are placed at a distance of 77cm from the plate. The stereo cameras have an interocular distance of 6.5cm and the cyclopean camera is placed in the middle of the left and right cameras. Figure 3(b) shows the distance of observation, and the display area to visualize the virtual plates. The field of view, fov , of the camera was calculated using the observation distance, a , and the width of the area of projection, b , $fov = 2 \times \arctan\left(\frac{2a}{b}\right)$.

4 USER STUDY

We designed a user study with 26 subjects using experimental design theory to optimize the number of trials run in order to obtain valid results using a minimum parameters variation of flake density and flake radius, see figure 5 (c). During the experiment, the subjects sat in a dark room, facing a stereoscopic screen. They observed two series of plates (stereoscopic/monoscopic),

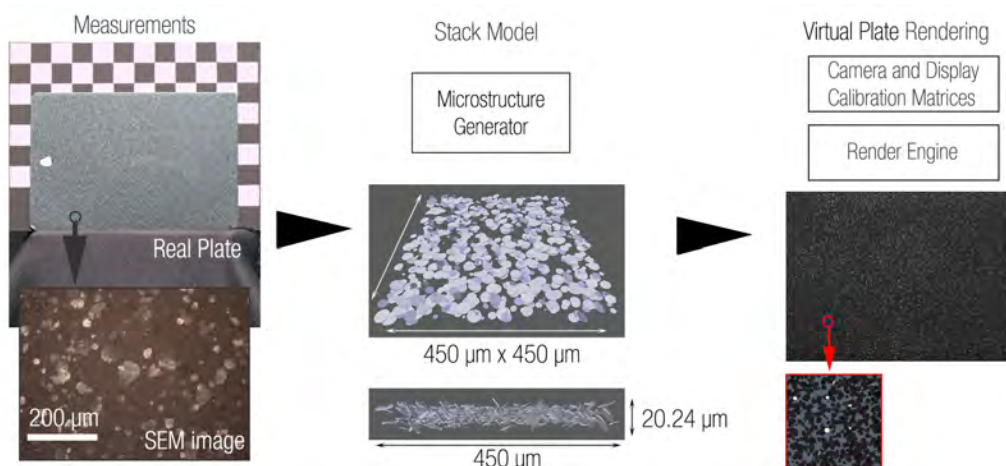


Figure 2: Through morphological and statistical analysis of SEM images, a set of microstructures are generated in order to fill the surface of the virtual plate. Then, the render engine computes the appearance of the virtual plate using the information of the microstructures, and the colorimetric calibration matrices of the photographic camera and the screen display used during the experiment.

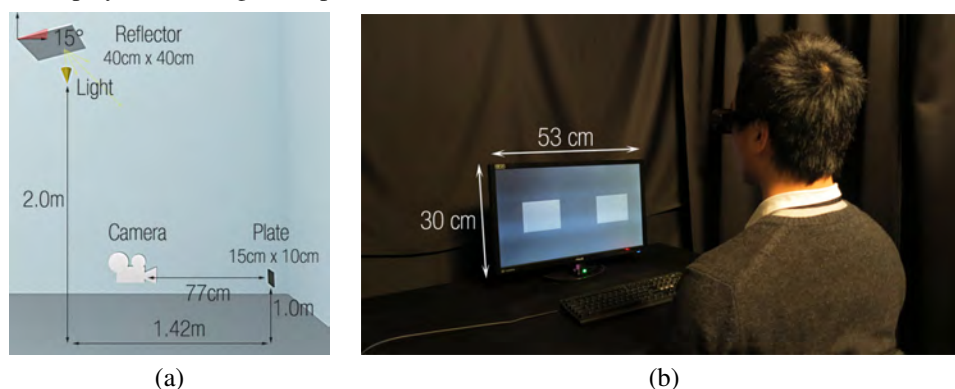


Figure 3: The image (a) is a schematic diagram used for the virtual scene. (b)The physical observation conditions to visualize the virtual plates.

Factor	Low Level	High Level	Physical Value
Flake Density	3.5	9.5	1.0
Metallic Flake Radius	15μm	45μm	30μm

Table 1: Based on the morphological and statistical analysis of the actual automotive paint, the flake radius is 30μm, and flake density is 1.0 (this value is unitless). The minimum and maximum range for flake density, and flake radius were found empirically. Within each interval, 13 values were chosen through Central Composite Design.

each one with different flake density and flake radius, see table 1. Subjects evaluated the similarity of the virtual plate to the photograph of the actual plate by using a scale from 0 (equal to the reference plate) to 10 (different from the reference plate). After an answer was given, the subject changed to the next plate with different radius and density of metallic flakes. For each trial, the presentation order of the stimuli follows a Williams Latin Square Design. The main experiment was preceded by a practice trial of two stimuli to gain familiarity with the experience.

The subjects used stereoscopic active shutter glasses during both monoscopic and stereoscopic conditions. For each trial, the subjects observed two sequences of 13 stereoscopic images. The first sequence corresponds to the monoscopic-condition, while the second corresponds to the stereoscopic case. In all experiments, the subjects used stereoscopic active shutter glasses NVIDIA 3D Vision 2 during both monoscopic and stereoscopic conditions. For the monoscopic conditions the same image was displayed for both eyes. The images were displayed using an active stereo ASUS VG248QE display. The stimulus was displayed with

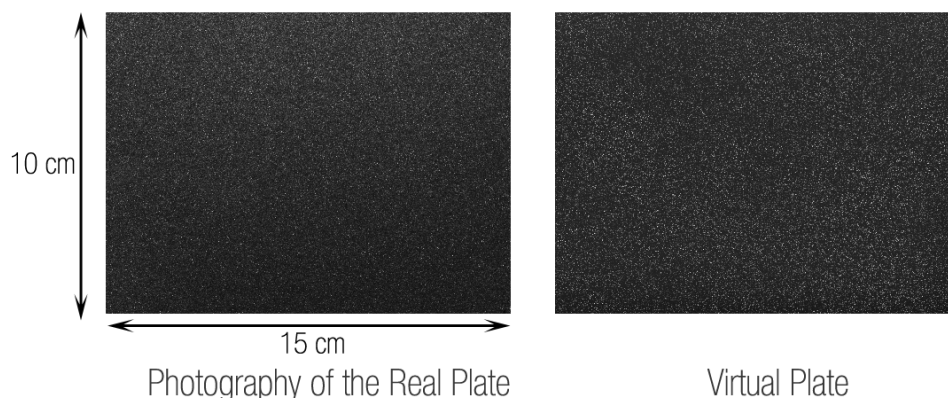


Figure 4: The stimulus displayed to the subjects. The "Reference" material (left plate) is static through the experiment, while the material of the plate "Sample" (right plate) changes according to 13 different values of flake densities, and flake radius size.

a resolution of 1920×1080 pixels at 72Hz. The stimulus consisted of two plates designated as reference, and variable plate, see figure 4. The reference is the photography of the actual automotive paint plate, which was taken with a camera *NikonD800*. The initial high dynamic range (HDR) image was made by taking 6 images with film sensitivity ISO 100, and the following shutter speeds: 1.3, 1.6, 2.0, 2.5, 3.0, and 4.0 seconds. Then, the HDR image was converted to the RGB colour space using the calibration matrices of the photographic camera, and the screen display. The plates dimensions are 10cm \times 15cm. The samples are placed inside of a dark room with one source of light SOLUX 4700K with known spectrum. The virtual stereo and cyclopean cameras are located at 77cm from the plate, which is the same distance of observation that was used to take the photography of the real plate.

5 RESULTS

5.1 Data Exploration

From the box plots, we noticed that there are some extreme outliers and extreme values. This is due to the fact that there is an important agreement within the population to give the same evaluation to a given plate. This is translated into a positive Kurtosis. A principal component analysis (PCA) was applied in order to verify if the observers generally agree in their evaluations. The first axis represents more than 80% in the two studies that is to say that there is an extraordinary agreement between the subjects. Thanks to these preliminary analyses, the average of the panel represents well the raw data so this indicator can be used in Data Modeling.

5.2 Data Modeling

The experimental design allows to evaluate the interaction between the two parameters, non linear effects, and to find the optimum values for each parameter. As we

said in the previous section, we can consider that the average of response is representative of the population. Therefore, we can model the response according to the parameters of the experimental design: linear and non linear effects of density and radius size, and their interaction. The surface of response depicted in figures 5 (a) and (b) have a bell shape surface. Hence, there is no interaction between the two factors: flake density and flake radius size. For the stereoscopic case we obtain a better R^2 pred (based on cross validation) and a smaller PRESS (Predicted Residual Sum of Squares), see table 3, therefore the stereoscopic model is more robust. The average degree of proximity to the photography of the actual sample is 5.1, and 4.6, for monoscopic and stereoscopic. The analysis of the quadratic effects show that for low or high density of flakes, the virtual plate is not considered similar to the real plate. The same result was found for small and large flakes radius. Finally, the Least Square Difference Test (LSD) show that with the stereoscopic condition the observers were able to discriminate better the plates.

6 DISCUSSION

There is a difference between the the monoscopic and stereoscopic observations of the plate. In average, the stereoscopic images of the virtual plate were better evaluated. The ANOVA repeated measure analysis on the global response indicates that the stereoscopic visualization of the virtual plate is closer to the actual plate. In other words, there is a better visual agreement to the photography of the physical plate with stereoscopic vision. Furthermore, the second ANOVA analysis on stereoscopic and monoscopic condition, confirms that the stereoscopic vision allows a better differentiation of the virtual plates. With monoscopic vision it is more perceptible the individual white reflections of the metallic flakes, and also the visual patterns resulted from the clustering of metallic flakes. While with the

	Coefficient		Signif. %	
	Monoscopic	Stereoscopic	Monoscopic	Stereoscopic
b_0	2.723	2.423	< 0.01***	< 0.01***
Radius Size b_1	-0.590	-0.730	< 0.0927***	< 0.0857***
Radius Size $b_1 - 1$	6.003	5.323	< 0.001***	< 0.001***
Flake Density b_2	-0.794	-0.516	< 0.0294***	0.318**
Flake Density $b_2 - 2$	1.810	1.822	< 0.001***	0.0123***

Table 2: The table of coefficients.

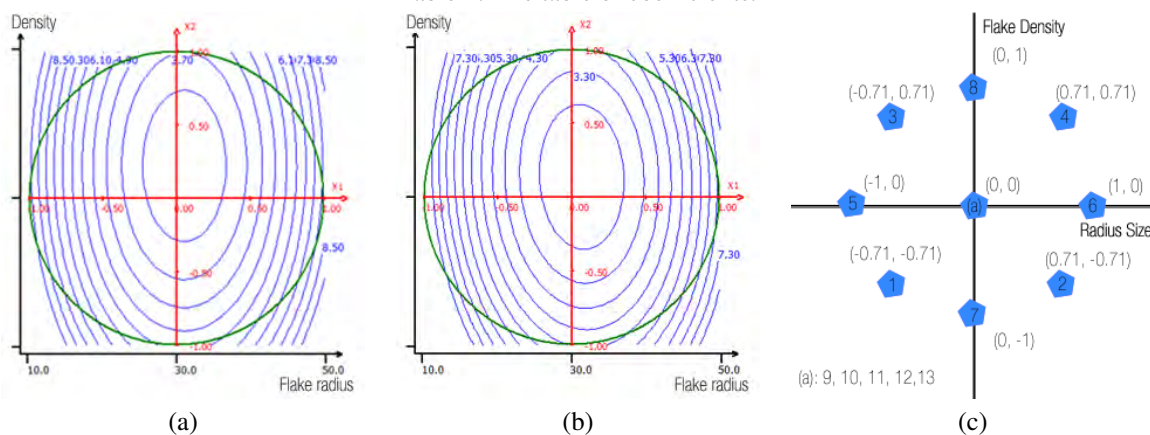


Figure 5: The graphs (a) and (b) depict the response surface of the experiment. (c) is the composite design used in the experiment that shows how many different plates to use and the variation of density and size of the metallic flakes. The values depicted in the graph of surface of responses are reduced and centered to the interval -1 to 1 so the influence of the factors can be compared. In this way, we can represent the domain of each factor in the same reference.

	Monoscopic	Stereoscopic
R2	0.961	0.976
R2 pred	0.726	0.838
PRESS	19.494	9.116

Table 3: The adequacy measures for the model.

stereoscopic vision it is more difficult to identify these patterns effects due to the binocular rivalry. Instead we can observe a glittering effect, which according to the comments of the observers, make the virtual plates to look more realistic.

In our experiments, we found that the radius of the flake has a great impact in the judgment of similarity. In figures 5 (a) and (b), the ellipsoidal shape of the isometric curve is oriented in the x_2 axis. This particular orientation shows that the quadratic effects are stronger in the x_1 axis, i.e., the flakes radius size axis. This dissymmetry is an indicator that the similarity evaluation note is more sensible to the radius size than to the flake density factor. In addition, according to the table of coefficients 2, the flake radius, $b_1 - 1$, is three times more important than the flake density, $b_2 - 2$. In the stereoscopic case, the shape of the isometric curve is tilted to the right. However, the radius size factor remains more sensible or influent than the flake density parameter.

From the obtained results, there are not particular tuples of factors that makes the subject to judge that the

virtual plate is similar to the photography, for instance a tuple with a large flake radius, and a strong flake density. For the monoscopic condition, the optimum values calculated from the surface response, show that in order the virtual plate to be considered similar to the photography, the plate must contain flakes with smaller radius size and to have a higher flake density. While in the stereoscopic condition, the optimum values show the inverse, higher flake radius size with lower flake density.

7 CONCLUSIONS

In this work, we evaluated the pertinence of a "virtual material workshop" approach, and the role of stereoscopy on perception of materials that depict binocular differences such as automotive paints with metallic flakes. For this purpose, we developed a user study based on a design of experiments, to evaluate the visual agreement between the observation of a computer generated object and the actual object. The results show that there is a match between the real and virtual metrics. This means that for a desired appearance our methodology can predict the microstructure. Secondly, the stereoscopic vision improves the visual representation of the virtual plates with metallic flakes. Finally, the size of flake radius has a great influence in the judgment of the observers.

We are currently working on the visualisation of virtual materials with a High Dynamic Range display, to study the influence of the high dynamic luminance on the perception of materials such as car paints. The next step for evaluating VR is to assess the pertinence of using head tracking to generate correct dynamic perspectives.

8 ACKNOWLEDGMENTS

This work is part of the LIMA project (Light Interaction Material Aspect), which is a collaborative research project between academic researchers and industrial manufacturers. The project is funded by the French National Research Agency, ANR, with the Grant Number ANR-11-RMNP-0014. The authors wish to thank F. Willot, E. Couka, D. Jeulin, and P. Callet for the microstructure models, A. Thorel, A. Chesnaud, and M. Ben Achour for the SEM measures, P. Porral for providing PSA Peugeot Citroën paint samples, and the persons who participated in the user study.

9 REFERENCES

- [1] Wilkie, A., Weidlich, A., Magnor, M., and Chalmers, A., “Predictive rendering,” in [ACM SIGGRAPH ASIA 2009 Courses], SIGGRAPH ASIA '09, 12:1–12:428, ACM, New York, NY, USA (2009).
- [2] Ulbricht, C., Wilkie, A., and Purgathofer, W., “Verification of physically based rendering algorithms,” *Computer Graphics Forum* **25**(2), 237–255 (2006).
- [3] Rushmeier, H., [Computer Graphics Techniques for Capturing and Rendering the Appearance of Aging Materials], 283–292, Springer US (2009).
- [4] Enguerrand Couka, François Willot, D. J., “A mixed boolean and deposit model for modeling of metal flakes in paint layers,” *Image Anal Stereol* **32**(2), 8–13 (2012).
- [5] Nicodemus, F. E., Richmond, J. C., Hsia, J. J., Ginsberg, I. W., and Limperis, T., “Radiometry,” ch. Geometrical Considerations and Nomenclature for Reflectance, 94–145, Jones and Bartlett Publishers, Inc., USA (1992).
- [6] Boher, P., Leroux, T., and Bignon, T. *SID Conference Record of the International Display Research Conference*.
- [7] Kook Seo, M., Yeon Kim, K., Bong Kim, D., and Lee, K. H., “Efficient representation of bidirectional reflectance distribution functions for metallic paints considering manufacturing parameters,” *Optical Engineering* **50**(1), 013603–013603–12 (2011).
- [8] Jensen, H. W., Marschner, S. R., Levoy, M., and Hanrahan, P., “A practical model for subsurface light transport,” in [Proceedings of the 28th Annual Conference on Computer Graphics and Interactive Techniques], SIGGRAPH '01, 511–518, ACM, New York, NY, USA (2001).
- [9] Ďurikovič, R. and Martens, W. L., “Simulation of sparkling and depth effect in paints,” in [Proceedings of the 19th spring conference on Computer graphics], SCCG '03, 193–198, ACM, New York, NY, USA (2003).
- [10] Ershov, S., Ďurikovič, R., Kolchin, K., and Myszkowski, K., “Reverse engineering approach to appearance-based design of metallic and pearlescent paints,” *Vis. Comput.* **20**, 586–600 (Nov. 2004).
- [11] Günther, J., Chen, T., Goesele, M., Wald, I., and Seidel, H.-P., “Efficient acquisition and realistic rendering of car paint,” in [Vision, Modelling, and Visualization 2005 (VMV), Proceedings, November 16-18, Erlangen, Germany], Greiner, G., Hornegger, J., Niemann, H., and Stamminger, M., eds., 487–494, Akademische Verlagsgesellschaft Aka GmbH, Berlin (November 2005).
- [12] Rump, M., Müller, G., Sarlette, R., Koch, D., and Klein, R., “Photo-realistic rendering of metallic car paint from image-based measurements,” *Computer Graphics Forum* **27**(2), 527–536 (2008).
- [13] Sung, L., Nadal, M. E., McKnight, M. E., Marx, E., and Dutruc, R., “Effect of aluminum flake orientation on coating appearance.” 1–15 (2001).
- [14] LEVELT, W. J. M., “Binocular brightness averaging and contour information,” *British Journal of Psychology* **56**(1), 1–13 (1965).
- [15] Ged, G., Obein, G., Silvestri, Z., Le Rohellec, J., and Viénot, F., “Recognizing real materials from their glossy appearance,” *Journal of Vision* **10**(9) (2010).
- [16] Obein, G., Knoblauch, K., and Viénot, F., “A framework for the measurement of visual appearance,” *Commission Internationale de l’Eclairage (CIE)* **4**, 711–720 (Aug. 2006).
- [17] Templin, K., Didyk, P., Ritschel, T., Myszkowski, K., and Seidel, H.-P., “Highlight microdisparity for improved gloss depiction,” *ACM Trans. Graph.* **31**, 92:1–92:5 (July 2012).
- [18] Wendt, G., Faul, F., and Mausfeld, R., “Highlight disparity contributes to the authenticity and strength of perceived glossiness,” *Journal of Vision* **8**(1) (2008).
- [19] Obein, G., Knoblauch, K., and Viénot, F., “Difference scaling of gloss: nonlinearity, binocularity, and constancy,” *Journal of vision* **4**, 711–720 (Aug. 2004).
- [20] Sakano, Y. and Ando, H., “Effects of head mo-

- tion and stereo viewing on perceived glossiness,” *Journal of Vision* **10**(9), 1–14 (2010).
- [21] David C. Knill, J. A. S., “Do humans optimally integrate stereo and texture information for judgments of surface slant?,” (2003).
- [22] McCamy, C. S., “Observation and measurement of the appearance of metallic materials. part i. macro appearance,” *Color Research and Application* **21**(4), 292–304 (1996).
- [23] McCamy, C. S., “Observation and measurement of the appearance of metallic materials. part ii. micro appearance,” *Color Research and Application* **23**(6), 362–373 (1998).
- [24] Fettis, G., [*Automotive Paints and Coatings*], Wiley (2008).